REINFORCEMENT OF ANTIMICROBIAL ACTIVITY AND SWELLING ABILITY OF STARCH-G-POLY 4-ACRYLAMIDOBENZOIC ACID USING CHITOSAN NANOPARTICLES

NAHED A. ABD EL-GHANY,[*] MOHAMED S. ABDEL AZIZ,[*]
MARWA M. ABDEL-AZIZ[**] and ZAIN M. MAHMOUD[*]

[*]*Cairo University, Faculty of Science, Chemistry Department, Giza 12613, Egypt*
[**]*El Azhar University, Regional Center for Mycology and Biotechnology, Egypt*
✉ *Corresponding author: N. A. Abd El-Ghany, dr_nahed_055@yahoo.com*

Received May 25, 2023

New nanocomposites, denoted as St-g-P4ABA/CSNPs1% and St-g-P4ABA/CSNPs3%, were created by combining starch-grafted polyacrylamide benzoic acid (St-g-P4ABA) with chitosan nanoparticles (CSNPs) (1% and 3% based on graft weight). Nuclear magnetic resonance (1H NMR), Fourier-transform infrared spectroscopy (FTIR), scanning electron microscopy (SEM), transmission electron microscopy (TEM), and X-ray diffraction were used to clarify the successful synthesis of the nanocomposite. The thermal stability of St-g-P4ABA copolymer and its degree of swellability in both water and 0.9% saline solutions significantly improved as a result of the incorporation of CSNPs, most notably in the saline solution. When compared to St-g-P4ABA, the St-g-P4ABA/CSNP composites showed better antibacterial activity against Gram-positive bacteria, Gram-negative bacteria and fungi.

Keywords: starch, nanochitosan, swellability, antimicrobial activity, minimum inhibitory concentration

INTRODUCTION

Due to its ingrained biodegradability, and the great abundance and annual renewability of its sources of extraction, starch is one of the most promising natural polymers. As it is cheap and can be handled using standard plastic processing mechanization, starch provides an attractive low-cost base for new biodegradable materials.[1]

Starch granules are constituted of two main fragments: amylose, a type of linear polymer of glucose units with α-(1→4) linkage, and amylopectin, which is substantially branched with a large number of short chains that are linked via α-(1→6) linkage to the linear parts of the macromolecule. Due to technological developments, the application field of starch is being extended gradually, and different techniques have been developed for the modification of starch to overcome its shortcomings.[2,3] These include poor processability and solubility in prevalent organic solvents, deterioration, low shear stress resistance, and thermal degradation. In addition, starch has no antimicrobial activity towards microorganisms.[4] Chemical and physical modifications of starch can provide more possibilities for the functionalization of starch and therefore expand its application scope. Further, various starch-based blends and biocomposites have been generated that exhibit improved performance.[5]

Recently, remarkable attention has been focused on the use of nanosized fillers in a starch matrix to form nanocomposites with enhanced mechanical properties compared to usual microcomposites.[6–9] This is because filler molecules at nanoscale sizes can form molecular bridges inside the polymer matrix. There are three distinct types of nanofillers: nanoparticles, nanotubes, and nanolayers.[10] Incorporating appropriate nanoparticles into starch as a biopolymer with complicated structures and specific properties will result in a new class of polymer nanocomposites developed for a wide range of both conventional and emerging applications.[11]

Chitosan, is an α (1-4) 2-amino-2-deoxy β-D glucan, obtained by the deacetylation of chitin, which is present in the exoskeleton of crustacean and several other organisms as insects and

fungi.[12] Chitosan nanoparticles (CSNPs) are primarily used due to their well-known polymeric and cationic properties.[13,14] Due to their small size, accessibility, lack of toxicity, and antibacterial qualities, chitosan nanoparticles (CSNPs) are an attractive choice for use as a biomaterial in biological applications.[15,16] The ionic gelation technique, emulsion crosslinking, spray drying, and emulsion-droplet coalescence are a few of the approaches that have been studied by several research teams to prepare chitosan nanoparticles.[16,17,18] Starch and chitosan work together synergistically in their nanocomposites, and it was fascinating to observe that the inclusion of starch grains boosts the mechanical strength of chitosan-TPP beads.[19] Chitosan and starch have been shown to interact with one another intermolecularly in their combination.

4-Aminobenzoic acid (4-ABA) and its derivatives have drawn a lot of pharmacological and commercial attention due to their well-known chemical characteristics and wide range of biological actions. 4-ABA is widely spread in nature and is present in large amounts in a variety of plant and animal tissues. It frequently serves as a structural component in pharmaceuticals and serves an essential pharmacophore role. In a large database of pharmaceuticals used for commercial sale, the 4-ABA moiety was discovered in 1.5% of the cases. Numerous 4-ABA nucleated compounds exhibit potent antibacterial,[20,21] anticancer,[22] antioxidant,[23] and immunomodulatory[24] properties. Additional properties of 4-ABA molecules include antineoplastic, anaesthetic, antiarrhythmic, anticonvulsant, antiemetic, and gastrokinetic properties.[25]

In our previous published work on the starch-acrylamidobenzoic acid composite,[25,26] the developed material showed improved swelling and antimicrobial properties, which encouraged us to study the effect of the incorporation of nanochitosan into the starch-acrylamidobenzoic acid matrix for further enhancement of the starch's inherent properties. The effect of the impregnated chitosan nanoparticles on the physical and chemical structure of starch was studied. The structure of the prepared nanocomposite was characterized by FTIR, 1H NMR, SEM, TEM, and TGA. The antimicrobial activity and the swelling behaviour of the prepared modified starch nanocomposites were also studied.

EXPERIMENTAL

Materials

Starch was purchased from Nasr Chemical Co., Egypt. 4-Aminobenzoic acid was purchased from Loba Chemie. Solvents, reagents, and all other chemicals were obtained from Aldrich and used as received. The microorganisms used for both antibacterial and antifungal activities were provided by the Regional Centre for Mycology and Biotechnology, Egypt.

Experimental methods

Synthesis of 4-acrylamidobenzoic acid

4-Acrylamidobenzoic acid (4-ABA) was synthesized using the same method as described in our previous publication.[25] Accordingly, a predetermined amount of acryloyl chloride (0.05 mol/L) was slowly added to a solution of 4-aminobenzoic acid (0.05 mol/L in DMF), the mixture was kept in an ice bath on a magnetic stirrer for 3 h. The reaction mixture was poured onto crushed ice to precipitate the crude product, which was then filtered, washed with cooled water, recrystallized in hot water, and finally dried in an oven at 60 °C for 8 h.

Synthesis of St-g-P4ABA/CSNPs composite

A predetermined amount of dry corn starch was dissolved in double-distilled water in a three-necked round-bottom flask, with a 1:50 liquor ratio and heated at 85 °C for 30 min with continuous stirring to obtain gelatinized corn starch. The reaction temperature was decreased to 65 °C, and a calculated amount of 4-acrylamidobenzoic acid (0.25 mol/L) was slowly added to the reaction mixture. The flask was placed in a water bath at 65 °C, and nitrogen gas was bubbled for 30 min under stirring to remove the dissolved oxygen. A predetermined amount of CSNPs was added to the reaction mixture. The graft copolymerization reaction was initiated by the slow addition of $3x10^{-2}$ mol/L of $(NH_4)_2S_2O_8/NaHSO_3$ as a redox initiator. The grafting process continued for 2 h and was terminated by the slow addition of cold methanol to precipitate the grafted nanocomposite, which was separated by filtration, washed several times with methanol, and then dried in an oven at 50 °C for 8 h. Two concentrations of the CSNPs were used (1% and 3% based on starch weight) to produce two starch nanocomposites, designated as P4ABA/CSNPs1% and P4ABA/CSNPs3%. The purification of the resultant nanocomposite from the homopolymer was performed by extraction with methanol using a Soxhlet apparatus for 8 h.[25] A schematic representation for the preparation of the St-g-P4ABA/CSNPs composite is illustrated in Scheme 2.

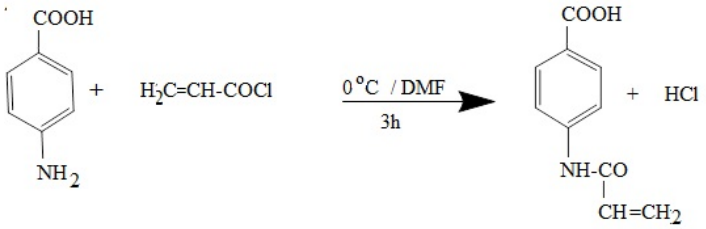

Scheme 1: Schematic representation of 4-ABA preparation

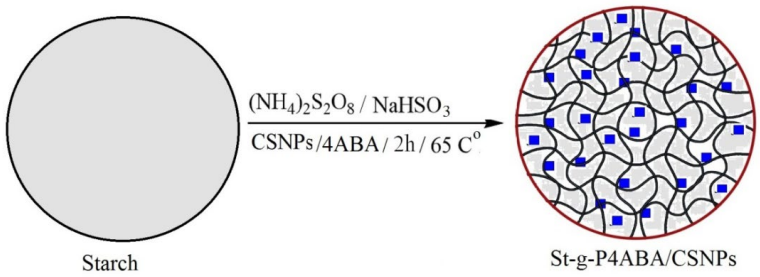

Scheme 2: Schematic representation for preparation of St-g-P4ABA/CSNPs composite

Grafting parameters, such as grafting percentage (%G), grafting efficiency (%GE), and homopolymer percentages (%H) were determined as follows:

$$\%G = [(W_2 - W_o)/W_o] \times 100 \quad (1)$$

$$\%GE = [(W_1 - W_o) / (W_2 - W_o)] \times 100 \quad (2)$$

$$\%H = [(W_1 - W_2) / W_3] \times 100 \quad (3)$$

where W_o is the initial starch weight, W_1, and W_2 are the weight of the grafted matrix before and after purification, respectively, and W_3 is the weight of the monomer charged.

RESULTS AND DISCUSSION

St-g-P4ABA/CSNP composites were synthesized and characterized; the impact of incorporating chitosan nanoparticles into the grafted starch matrix was studied. The results showed improvements in thermal stability, swellability, and antimicrobial activity.

Characterization

FTIR analysis

Figure 1 shows the FTIR spectra of free starch and St-g-P4ABA/CSNP composites. The free starch spectrum exhibited a characteristic broad band at 3431 cm^{-1} related to stretching vibrations of OH groups, and broad bands at 2928 and 1428 cm^{-1} were attributed to the stretching and bending vibrations of CH_2 groups, respectively. The low-intensity band at 1640 cm^{-1} is due to protein and fat contamination. The characteristic bands of C-O-C, C-C, and C-OH were observed at 1157 cm^{-1}, 1082 cm^{-1}, and 1017 cm^{-1}, respectively, while the observed band at 857 cm^{-1} is related to the glucopyranose ring.[25-27]

The spectra of St-g-P4ABA showed that, in addition to the characteristic bands of starch, new bands appeared at 1752, 1683, and 1653 cm^{-1} attributed to stretching vibrations of the carboxylic C=O group, amide C=O and bending NH group, respectively. The two bands at 1598 and 1534 cm^{-1} are due to the C=C vibration of the benzene ring. Moreover, the band at 768 cm^{-1} is due to the para-substituted benzene ring.

The spectra of St-g-P4ABA/CSNP nanocomposites showed, in addition to the characteristic bands of both starch and 4ABA, an increase in the intensity of the peak around 3431 cm^{-1} due to the additional NH and OH groups of the CSNPs. Another new broad band around 1255 cm^{-1} was observed, corresponding to the P-O bond of TPP in the prepared CSNPs. The ionic interaction between the CSNPs and the grafted polymer was evidenced by the lower shift in many vibration frequencies, since the stretching vibration of the NH group at 3426 cm^{-1} was shifted to 3414 and 3410 cm^{-1}, while the stretching vibration of the carboxylic C=O group and the amide C=O group was overlapped and shifted to 1695 and 1693 cm^{-1} in the spectra of St-g-P4ABA/CSNPs1% and St-g-P4ABA/CSNPs3%, respectively, which confirms the formation of the nanocomposites.

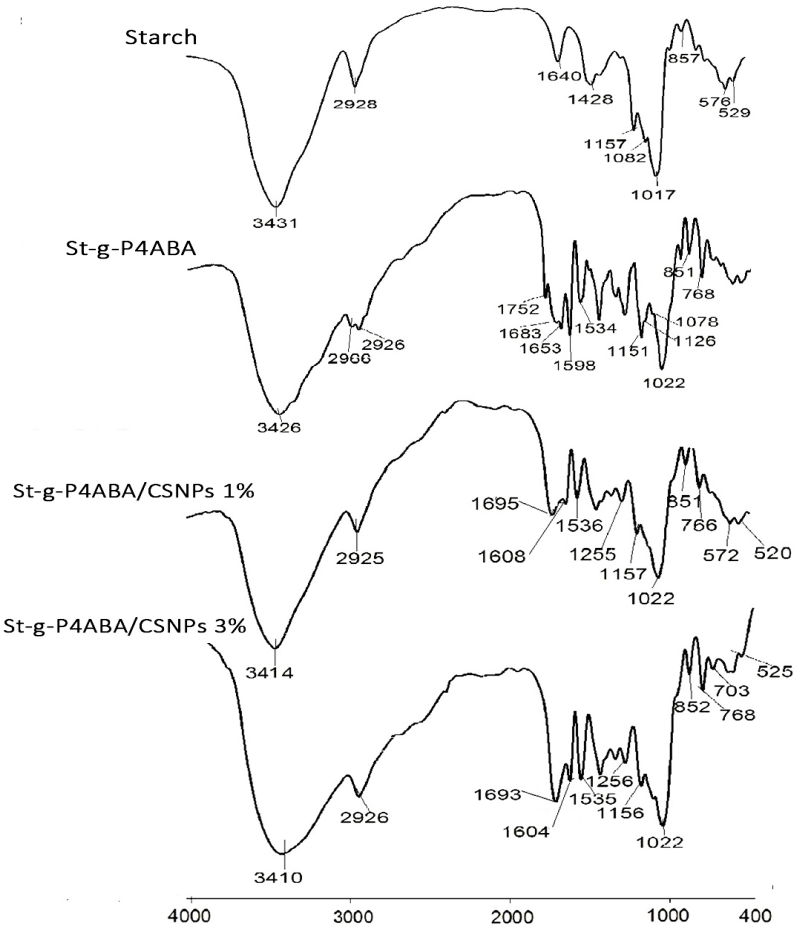

Figure 1: FTIR spectra of starch, St-g-P4ABA, St-g-P4ABA/CSNPs1% and St-g-P4ABA/CSNPs3%

[1]H NMR analysis

Figure 2 shows the 1H NMR spectrum of the St-g-P4ABA/CSNPs composite (St-g-P4ABA/CSNPs3% as a representative example), which displays characteristic data as described further. The signal at 3.624 ppm is related to the protons of carbons 2, 3, 4, and 7 of the pyranose ring; the signals at 4.543 ppm and 4.868 ppm refer to the protons of carbons 6 and 5, respectively. The signal at 5.431 ppm is attributed to the protons of carbons 1 and 8, while the multiplet at 7.509–7.686 ppm represents the protons of the para-substituted benzene ring. The broad signal at 9.920 ppm is assigned to the NH of the amide group, while the signal at 10.015 ppm is related to the chitosan amino group (NH2, 2H). The broad peak at 11.8 ppm is related to the -COOH protons. The reported data confirm the successful formation of St-g-P4ABA/CSNP composites.

Powder X-ray diffractometry

In the XRD pattern of the corn starch (Fig. 3), four major characteristic crystalline peaks were observed at 2Θ = 15.2°, 16.9°, 18.2° and 23.2°, which indicate crystallization.[25,26,28,29] The crystalline peaks shifted towards a lower angle and became weaker in the gelatinized corn starch pattern; it showed a new peak at 2Θ = 17.4° and the peak at 23.3° of lower intensity, while they disappeared entirely in the XRD pattern of the modified corn starch, St-g-P4ABA. Therefore, we deduced that the crystal structure of the original polymer was reduced in the gelatinized polymer, but destroyed in the St-g-P4ABA matrix. This result can be explained by the decrystallization effect of the incorporated grafting molecules, which disrupted the regularity of the polymer chains and the intramolecular hydrogen bonding in polymer molecules, resulting in significant changes in the polymer's crystalline structure. The St-g-P4ABA/CSNPs3% XRD pattern (St-g-P4ABA/CSNPs3% as a representative example) showed further irregularity and amorphousness of the polymeric inner structure, and the new peak that appeared at 2Θ =21.1° is related to the crystalline CSNP particles that are imbedded

inside the matrix. These results confirm the formation of the nanocomposite.

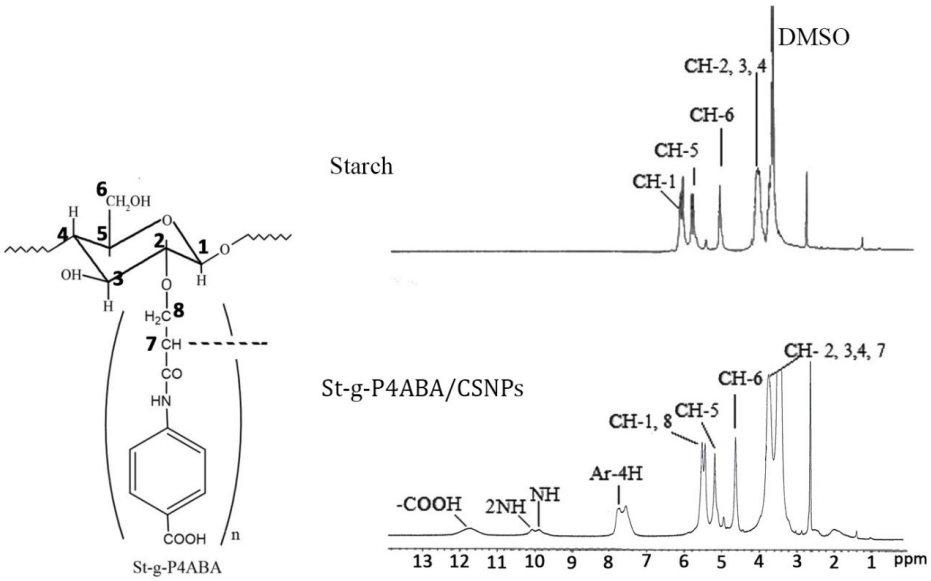

Figure 2: 1H NMR spectra of starch and St-g-P4ABA/CSNPs composite

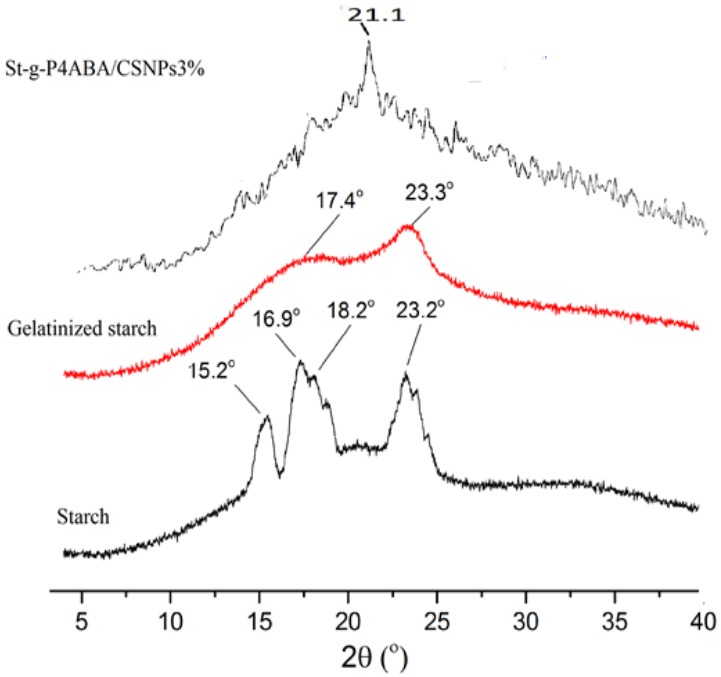

Figure 3: XRD patterns of starch, gelatinized starch and St-g-P4ABA/CSNPs 3%

Scanning electron microscopy (SEM) and transmittance electron microscopy (TEM) studies

SEM analysis showed the morphological structure of gelatinized starch, St-g-P4ABA, and St-g-P4ABA/CSNPs composite (St-g-P4ABA/CSNPs3% as a representative example). The images clearly demonstrated the change in surface topology. Compared to the smooth surface of gelatinized starch (Fig. 4a), the surface of St-g-P4ABA appeared full of lumps and large inner spaces between the polymer chains (Fig. 4b).[30] The SEM image of St-g-P4ABA/CSNPs revealed that the CSNPs were uniformly distributed on the surface and throughout the matrix, filling the inner space through ionic interaction with the polymer functional groups (Fig. 4c).

The TEM study, which showed the size and dispersion of the nanoparticles throughout the

matrix, validated the production of starch nanocomposites. The TEM pictures revealed that CSNPs, with diameters ranging from 80 to 100 nm, were uniformly distributed inside the polymeric matrix, and when the CSNP concentration increased from St-g-P4ABA/CSNPs1% to St-g-P4ABA/CSNPs3%, their distribution grew denser, as shown in Figure 5.

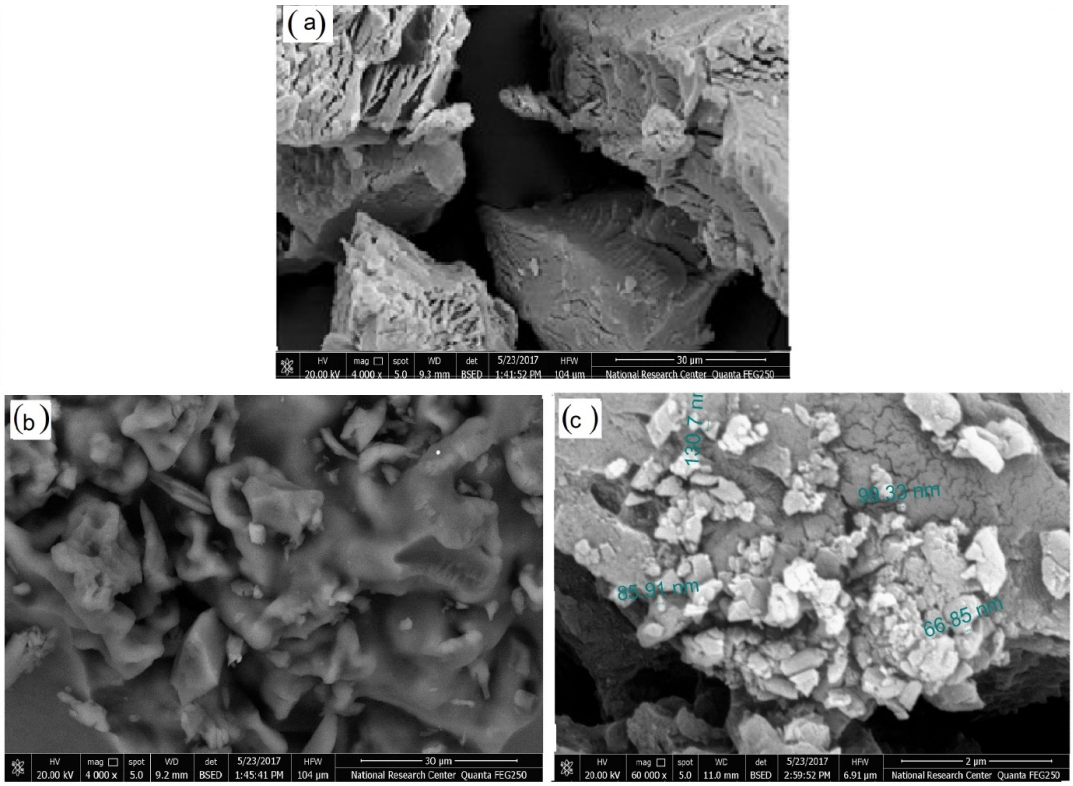

Figure 4: SEM images of (a) gelatinized starch, (b) St-g-P4ABA, and (c) St-g-P4ABA/CSNPs3%

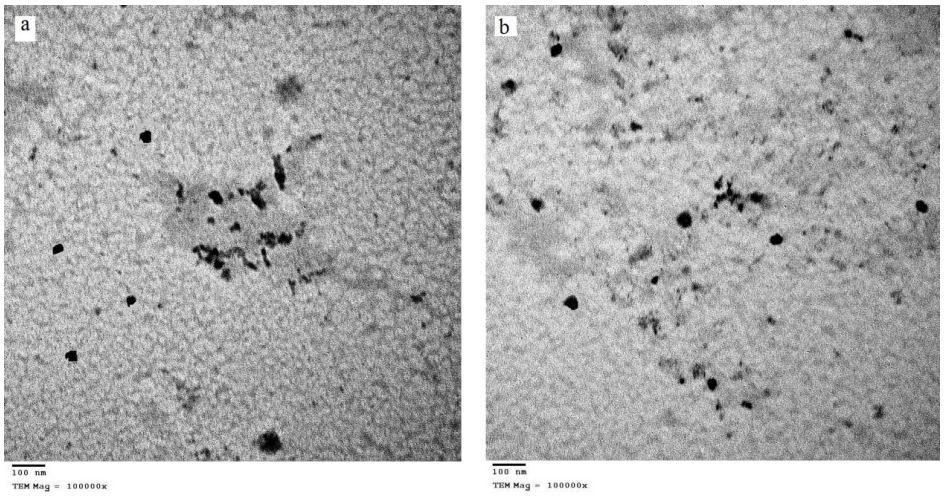

Figure 5: TEM images of (a) St-g-P4ABA/CSNPs1% and (b) St-g-P4ABA/CSNPs3%

Thermogravimetric analysis

Figure 6 (a, b) shows the TG and DTG curves of starch, St-g-P4ABA and St-g-P4ABA/CSNP composites. The thermal stability of corn starch and St-g-P4ABA was explained in our previous work,[25,31] which stated that the thermal stability of neat starch was improved after grafting, as judged from the lower mass loss of the grafted sample compared to the free starch at maximum degradation. The thermogram of St-g-P4ABA showed three degradation steps, the first ranging from 60 to 120 °C due to the removal of adsorbed

water, the second starting at 229 °C and attributed to degradation of the polymer backbone, while the grafted chains started decomposition at 350 °C due to the presence of the highly stable aromatic ring. The second degradation was shifted to a higher temperature (245 °C) in St-g-P4ABA/CSNPs composite thermograms, indicating more resistance to thermal degradation. These higher temperatures were reasonably attributed to the higher aspect ratio (width to thickness) of the nanofiller, acting as a heat barrier and, meanwhile, restricting the polymer chains' mobility.[32] Meanwhile, the ionic interaction between the CSNPs and the polymer functional groups resulted in the uniform distribution of the nanoparticles within the polymer matrix, which would mean a higher heat barrier and higher thermal stability of the nanocomposites. It is worth mentioning that, as the CSNPs' density increases, the mobility of the polymeric chains becomes more restricted due to thermal degradation. The observed degradation that extended from 350 to 450 °C was attributed to the degradation of the grafted molecules.

From the thermogram analysis, the residual masses at 500 °C were 33% and 38% for St-g-P4ABA/CSNPs1% and St-g-P4ABA/CSNPs3%, respectively, which corresponded to 40% for St-g-P4ABA. These lower residual masses of the nanocomposites resulted from the degradation of the CSNPs at elevated temperatures.

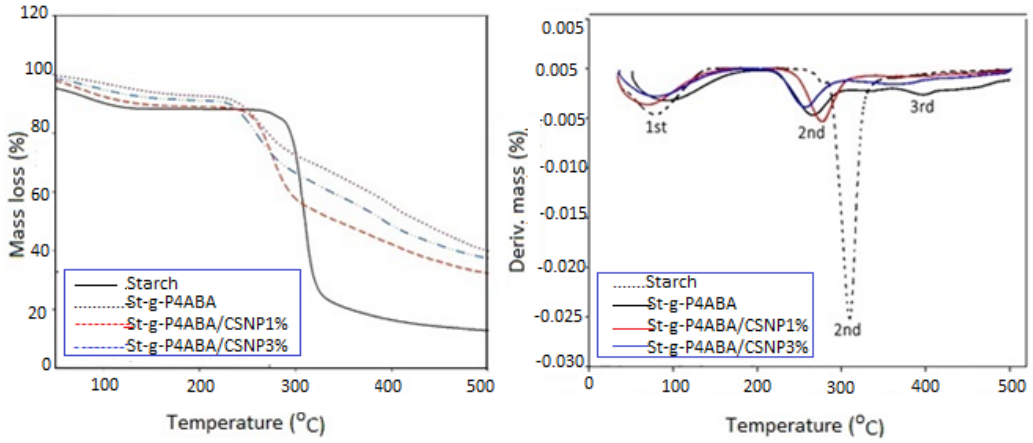

Figure 6: (a) TGA and (b) DTGA diagrams of starch, St-g-P4ABA, St-g-P4ABA/CSNPs1% and St-g-P4ABA/CSNPs3%

Swelling behavior of St-g-P4ABA/CSNP composites in water and 0.9% saline solution

It is well known that starch has hydrophilic OH groups, which allow it to swell in aqueous solutions to some extent, depending on the amount of the hydrophilic groups. The hydrophilic character of starch can be improved via grafting with molecules having hydrophilic function groups, such as COOH and NH_2 groups, which can form hydrogen bonds with the diffused solvent molecules.[25,26,33] Grafting 4-ABA on the starch backbone results in a significant increase in the swelling ability of starch. Two factors are responsible for the increased swellability: first, the breakdown of the intermolecular hydrogen bonds increased the polymeric matrix's internal space; and second, the incorporation of the COOH, CO, and NH groups increased the hydrophilic nature of native starch.[34] Also, the swelling ability percent of grafted starch in water and 0.9% saline solution appeared greater than that of free starch.[25,26,35] On the other hand, loading of CSNPs on St-g-P4ABA further increased the swelling capability in water and saline solution, which might be due to (1) the hydrophilic nature of nanochitosan due to the additional NH_2 groups, and (2) the increased surface area for absorption. It seemed from the results that the degree of swelling ability of St-g-P4ABA/CSNPs1% was greater than that of St-g-P4ABA/CSNPs3%; this might be due to the decrease in the free space inside the polymeric sample, as the amount of CSNPs increased. The recorded swelling data are summarized in Table 1.

Antibacterial study

The antibacterial activity of corn starch and starch derivatives was investigated by measuring their zone of inhibition on bacterial growth using

the agar diffusion method. *S. aureus* and *E. faecalis* were used as gram-positive bacteria for this investigation, while *K. pneumoniae* was used as gram-negative bacteria, and Ciprofloxacin was used as the standard drug. The results summarized in Table 2 revealed that starch has no antibacterial effect, as it exhibited zero inhibition,[25,26,36,37] while all prepared starch derivatives were more potent in inhibiting the growth of bacteria. Thus, the St-g-P4ABA sample exhibited inhibition zones of 14.1±2.1, 15.6±1.2 and 17.9±1.5 mm against *S. aureus*, *E. faecalis* and *K. pneumoniae*, respectively. The higher antimicrobial activity of grafted starch resulted from the presence of the polar groups (-COOH, CO, and NH groups of the grafted molecules), which increase the solubility of starch and facilitate the diffusion of the polymer inside the microorganism, thus enhancing the interaction with the bacterial cell membrane and altering their function, preventing the bacterial growth.

The antibacterial efficacy of St-g-P4ABA/CSNP composites was significantly increased. Since St-g-P4ABA/CSNPs1% recorded inhibition zones of 22.4±0.44, 20.6±0.63, and 21.7±0.19 mm against *S. aureus*, *E. faecalis* and *K. pneumoniae*, respectively, while St-g-P4ABA/CSNPs3% recorded inhibition zones of 22.5±1.2, 21.2±0.58, and 23.2±0.63 mm against the same strains. These values are very close and, in many cases, equal to those recorded for the standard drugs, since Ciprofloxacin recorded inhibition zones of 23.8±1.2, 27.4±0.72 and 23.4±0.63 mm against *S. aureus*, *E. faecalis* and *K. pneumoniae*, respectively. These results are well illustrated in Figure 7. The higher antibacterial activity of the prepared starch nanocomposites might result from a combination of several factors: (1) The incorporated CSNPs added new function groups (NH_2, OH, and P-O) to the polymer, thus increasing the chance of interaction with the bacterial cell membrane and increasing the ability to chelate with the metal of the nutrient responsible for bacterial growth, leading to bacterial death;[25,26,38,39] (2) CSNPs increase the surface area of interaction with the microbial membrane, leading to a higher inhibition effect. The slight difference in antibacterial efficiency of starch derivatives on both gram-positive and gram-negative bacteria resulted from their different cell membrane compositions.

Table 1
Swelling behaviour of starch, St-g-P4ABA, and St-g-P4ABA/CSNP composites in water and 0.9% saline solution

Sample	% G	% Water uptake	% Saline uptake
Starch	0	1406	1330
St-g-P4ABA	75	2298	2192
St-g-P4ABA/CSNPs1%	55	2538	2433
St-g-P4ABA/CSNPs3%	50	2490	2348

Antifungal study

The antifungal activity of starch, St-g-P4ABA and St-g-P4ABA/CSNP composites was studied using the agar-well diffusion method by measuring the diameter zone of inhibition against *A. fumigatus* and *C. albicans* using Amphotericin B as a standard drug for comparison. Table 2 shows the recorded inhibition zones. The results illustrated that free starch has no effect on the growth of fungi. In contrast, St-P4ABA exhibited efficient antifungal activity; it recorded inhibition zones of 16.8±1.2 and 14.3±1.5 mm against *A. fumigatus* and *C. albicans*, respectively, while the St-g-P4ABA/CSNP composites showed more potent antifungal activity as judged from their inhibition zone values. Specifically, St-g-P4ABA/CSNPs1% exhibited inhibition zones of 21.7±0.19 and 20.3±0.58 mm against *A. fumigatus* and *C. albicans*, respectively, and St-g-P4ABA/CSNPs3% displayed 23.2±0.63 and 21.4±1.2 mm against the same strains, very comparable to those recorded for the reference drug Amphotericin B (23.4±0.63 and 23.7±1.2 mm, respectively), as depicted in Figure 8. The higher antifungal activity of the nanocomposites might be due to a number of reasons:

1. The hydrophilic nature of the nanocomposites can facilitate their penetration inside the hyphae of fungi, interfering with the enzyme activity responsible for fungal growth;
2. Adsorption and immobilization of the fungi on the nanocomposite surface;[25,39]
3. The carboxylic group of the grafted molecules can bind physicochemically to ergosterol in the fungal membrane, altering its permeability and causing leakage of vital

cytoplasmic components, leading to fungal death.[25,26]

Table 2
Antimicrobial activity of starch, St-g-P4ABA and St-g-P4ABA/CSNP composites against *S. aureus*, *E. faecalis*, *K. pneumonia*, *A. fumigatus* and *C. albicans*

Tested microorganism	Inhibition zone (mm)				Standard antibiotic
Gram-positive bacteria	Starch	St-g-P4ABA	St-g-P4ABA/CSNPs1%	St-g-P4ABA/CSNPs3%	Ciprofloxacin
S. aureus (ATCC 25923)	0	14.1±2.1	22.4±0.44	22.5±1.2	23.8±1.2
E. faecalis (ATCC 29212)	0	15.6±1.2	20.6±0.63	21.2±0.58	27.4±0.72
Gram-negative bacteria					Ciprofloxacin
K. pneumoniae (ATCC BAA1705)	0	17.9 ±1.5	21.7±0.19	23.2±0.63	23.4±0.63
Fungi					Amphotericin B
A. fumigatus (ATCC 46645)	0	16.8±1.2	20.3±0.58	21.4±1.2	23.7±1.2
C. albicans (ATCC 24433)	0	14.3±1.5	21.3±0.58	22.5±1.5	25.4±0.58

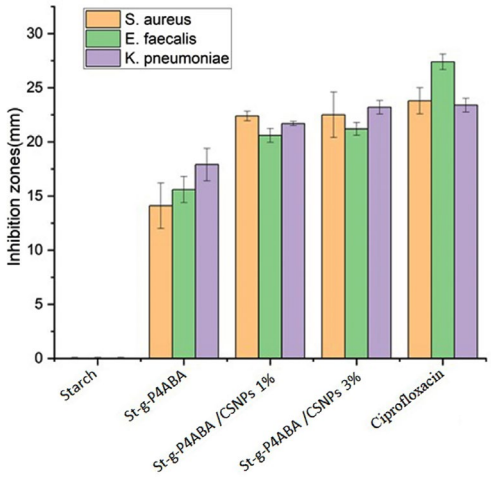

Figure 7: Inhibition zone diameter of starch, St-g-P4ABA and St-g-P4ABA/CSNPs composites against *S. aureus*, *E. faecalis* and *K. pneumoniae*

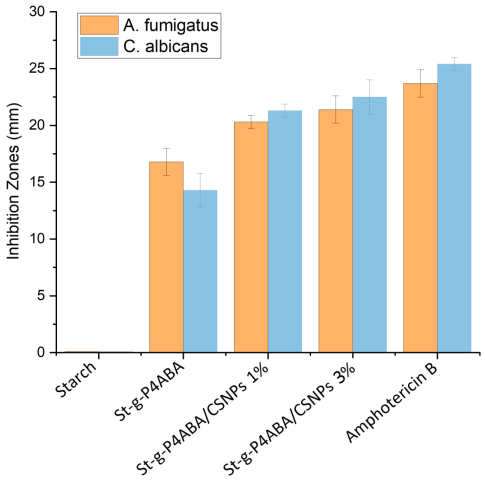

Figure 8: Inhibition zone diameter of starch, St-g-P4ABA and St-g-P4ABA/CSNPs composites against *A. fumigatus* and *C. albicans*

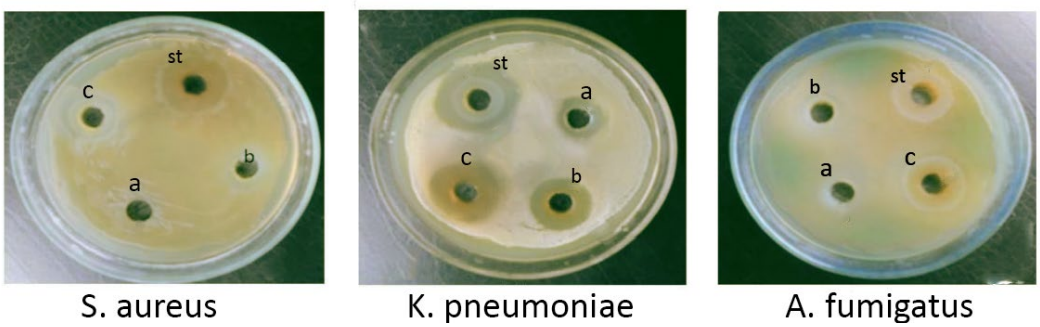

Figure 9: Photographs for the antimicrobial behaviour of (a) St-g-P4ABA, (b) St-g-P4ABA/CSNPs1%, (c) St-g-P4ABA/CSNPs3% against *S. aureus*, and *K. pneumonia*, in comparison with the antibacterial standard drug ciprofoxacin (st), and against *A. fumigatus* in comparison with the antifungal standard drug Amphotericin B (st)

Table 3
Minimum inhibitory concentration indices of St-g-P4ABA/CSNPs composites against *K. pneumoniae*, *E. faecalis*, *S. aureus*, *C. albicans* and *A. fumigatus*

Samples	Minimum inhibitory concentration ((MIC) µg/mL)				
	Tested bacteria			Tested fungi	
	K. pneumoniae	*E. faecalis*	*S. aureus*	*C. albicans*	*A. fumigatus*
St-g-P4ABA	7.8	31.25	62.5	31.25	31.25
St-g-P4ABA/CSNPs1%	1.95	3.9	1.95	3.9	1.95
St-g-P4ABA/CSNPs3%	1.95	3.9	1.95	3.9	1.95
Ciprofloxacin	0.98	0.49	0.49	-	-
Amphotericin B	-	-	-	0.49	0.98

Normal photographs were taken to illustrate the antimicrobial behaviour of the nanocomposites against selected microorganisms and displayed in Figure 9.

Minimum inhibitory concentration (MIC) measurements

The growth inhibition activity of the prepared samples against the tested microorganism was supported by measuring the minimum inhibitory concentration (MIC). The MIC is considered to be the lowest concentration that can completely inhibit inoculums compared with the control. Compared to St-g-P4ABA, the St-g-P4ABA/CSNP composites exhibited lower MIC values against the tested microorganisms, ranging from 1.95 to 3.5 µg/mL, which is comparable to that recorded by the standard drugs Ciprofloxacin and Amphotericin B, indicating the higher antimicrobial activity of the nanocomposites, as illustrated in Table 3.

CONCLUSION

Starch/poly 4-acrylamidobenzoic acid copolymer and nanochitosan were combined to create new nanocomposites, designated as St-g-P4ABA/CSNPs1% and St-g-P4ABA/CSNPs3%, based on the amount of the nanochitosan used. The FTIR and 1HNMR measurements provided proof that the nanocomposites had been successfully synthesized. Thermogravimetric testing revealed that the St-g-P4ABA/CSNP composites had greater thermal stability than native starch and the grafted copolymer St-g-P4ABA, demonstrating the stabilizing effect of chitosan nanoparticles on grafted starch. The higher degree of swellability of the St-g-P4ABA/CSNP composites in both water and saline solutions was due to the hydrophilic nature of the chitosan nanoparticles, which attached easily to the liquid molecules via the hydrogen bond and electrostatic interaction. Additionally, the antimicrobial behaviour of the prepared St-g-P4ABA/CSNP composites against different pathogens illustrated the inhibition potency of the St-g-P4ABA/CSNP composites towards the growth of the microorganisms, especially against *S. aureus*, *E. faecalis*, *K. pneumonia*, *A. fumigatus*, and *C. albicans*, as evidenced by the higher inhibition zone diameters and lower minimum inhibitory concentration values.

REFERENCES

[1] K. Encalada, M. Belén, E. Proaño and V. Valle, *Revista Ciencia e Ingeniería*, 39 245-258(2018)
[2] J. Chesterman and J. Kohn, in "Principles of Tissue Engineering", edited by R. Lanza, R. Langer, J. P. Vacanti and A. Atala, Academic Press, 2020, pp. 317-342, https://doi.10.1016/B978-0-12-818422-6.00019-8
[3] N. A. Abd El-Ghany, M. H. Abu Elella, H. M. Abdallah, M. S. Mostafa and M. Samy, *J. Polym. Environ*., **31**, 2792 (2023), https://doi.10.1007/s10924-023-02798-x
[4] L. García-Guzmán, *Polysaccharides*, **3**, 136 (2022), https://doi.org/10.3390/polysaccharides3010007
[5] N. R. Singha and P. K. Chattopadhyay, in "Biodegradable Polymers, Blends and Composites", edited by S. Mavinkere Rangappa, J. Parameswaranpillai, S. Siengchin, M. Ramesh, Woodhead Publishing Series in Composites Science and Engineering, Woodhead Publishing, 2022, pp. 205-236, https://doi.org/10.1016/B978-0-12-823791-5.00006-5
[6] A. D. de Oliveira and C. A. G. Beatrice, in "Nanocomposites", edited by S. Sivasankaran, IntechOpen, 2018, https://doi.org/10.5772/intechopen.81329
[7] S. Fakirov, *Adv. Mater. Lett*., **9**, 400 (2018), https://doi.org/10.5185/amlett.2018.1850
[8] S. Fu, Z. Sun, P. Huang, Y. Li and N. Hu, *Nano Mater. Sci*., **1**, 2 (2019), https://doi.org/10.1016/j.nanoms.2019.02.006
[9] N. H. Zakaria, N. Muhammad and M. M. A. B. Abdullah, in *IOP Conference Series: Materials Science and Engineering*, *International Conference on Innovative Research - ICIR Euroinvent 2017*, 25–26

May, 2017, Iasi, Romania, vol. 209, 012087 (2017), https://doi.10.1088/1757-899X/209/1/012087
[10] M. Mousa and Y. Dong, *Polymers* (*Basel*), **12**, 264 (2020), https://doi.org/10.3390/polym12020264
[11] A. Sarker, S. Chandra Mondal, R. Ahmmed, J. Rana, M. W. Rahman Ansary *et al*., in "Smart Polymer Nanocomposites", edited by N. Ali, M. Bilal, A. Khan, T. Anh Nguyen, R. K. Gupta, Elsevier, 2023, pp. 355-377, https://doi.org/10.1016/B978-0-323-91611-0.00021-9
[12] L. G. Confederat, C. G. Tuchilus, M. Dragan, M. Sha'at and O. M. Dragostin, *Molecules*, **17**, 3694 (2021), https://doi.org/10.3390/molecules26123694
[13] B. Brixner, C. M. da Silva, L. D. Pollo and J. D. Pollo Renner, *Res. Soc. Develop.*, **11**, 1 (2022), https://doi.org/10.33448/rsd-v11i14.36563
[14] T. Huqa, A. Khana, D. Brown, N. Dhayagude, Z. He *et al*., *J. Bioresour. Bioprod.*, **30**, 14 (2022), https://doi.10.1016/j.jobab.2022.01.002
[15] S. S. Al-Zahrania, R. Singh Borac and S. M. Al-Garni, *Biotechnol. Biotechnol. Equip.*, **1**, 1874 (2022), https://doi.10.1080/13102818.2022.2027816
[16] N. A. Abd El-Ghany and M. H. Abu Elella, in "Materials Science and Engineering in Food Product Development", edited by W. F. Lai, Wiley, 2023, Chapter 1, https://doi.org/10.1002/9781119860594.ch1
[17] A. Plucinski, Z. Lyu and B. V. K. J. Schmidt, *J. Mater. Chem. B*, **9**, 7030 (2021), https://doi.10.1039/d1tb00628b
[18] N. A. A. El-Ghany and M. A. H. Elella, "Food Packaging Films Generated From 2D Biopolymer-Based Nanocomposites", New York, Nova Science Publishers Inc., 2022
[19] M. C. Di Santo, C. L. D'Antoni, A. P. Domínguez Rubio, A. Alaimo and O. E. Pérez, *Biomed. Pharmacother.*, **142**, 111970 (2021), https://doi.org/10.1016/j.biopha.2021.111970
[20] X. Pan, Y. Zheng, R. Chen, S. Qiu, Z. Chen *et al*., *Cryst. Growth Des.*, **19**, 2455 (2019), https://doi.10.1021/acs.cgd.9b00137
[21] H. Veeravarapu, M. Tirumalasetty, S. P. Kurati, U. Wunnava and M. K. K. Muthyala, *Bioorg. Med. Chem. Lett.*, **30**, 127603 (2020), https://doi.10.1016/j.bmcl.2020.127603
[22] B. Sapijanskaitė-Banevič, V. Palskys, R. Vaickelionienė, J. Šiugždaitė, P. Kavaliauskas *et al*., *Molecules*, **26**, 2597 (2021), https://doi.org/10.3390/molecules26092597
[23] Y. V. Markitantova, S. I. Akberova, A. A. Ryabtseva and O. G. Stroeva, *Biol. Bull. Russ. Acad. Sci.*, **45**, 226 (2018), https://doi.10.1134/S1062359018020061
[24] M. Sowinska, M. Morawiak, M. Bochyńska-Czyż, A. W. Lipkowski, E. Ziemińska *et al*., *Biomolecules*, **9**, 89 (2019), https://doi.10.3390/biom9030089
[25] N. A. Abd El-Ghany, M. S. Abdel Aziz, M. M. Abdel-Aziz and Z. Mahmoud, *Int. J. Biol. Macromol.*, **134**, 912 (2019), https://doi.org/10.1016/j.ijbiomac.2019.05.078
[26] N. A. Abd El-Ghany and Z. M. Mahmoud, *Polym. Bull.*, **78**, 6161 (2021), https://doi.10.1007/s00289-020-03417-8
[27] M. Pirouzifard, R. Ashrafi Yorghanlu and S. Pirsa, *J. Thermoplast. Compos. Mater.*, **33**, 915 (2020), https://doi.10.1177/0892705718815541
[28] K. Dome, E. Podgorbunskikh, A. Bychkov and O. Lomovsky, *Polymers*, **12**, 641 (2020), https://doi.10.3390/polym12030641
[29] J. Xu, A. Blennow, X. Li, L. Chen and X. Liu, *Carbohyd. Polym.*, **229**, 115481 (2019), https://doi.10.1016/j.carbpol.2019.115481
[30] I. Chakraborty, S. Pallen, Y. Shetty, N. Roy and N. Mazumder, *Biophys. Rev.*, **12**, 105 (2020), https://doi.10.1007/s12551-020-00614-7
[31] Y. Liu, L. Yang, C. Ma and Y. Zhang, *Materials* (*Basel*), **12**, 699 (2019), https://doi.org/10.3390/ma12050699
[32] S. Zhang, J. Zhu, Y. Liu, S.-Y. Zou and L. Lin, *Polymers* (*Basel*), **11**, 342 (2019), https://doi.org/10.3390/polym11020342
[33] E. Motamedi, B. Motesharezedeh, A. Shirinfekr and S. M. Samar, *J. Environ. Chem. Eng.*, **8**, 103583 (2020), https://doi.org/10.1016/j.jece.2019.103583
[34] N. A. Mohamed and N. A. Abd El-Ghany, *Cellulose Chem. Technol.*, **50**, 463 (2016), https://www.cellulosechemtechnol.ro/pdf/CCT3-4(2016)/p.463-471.pdf
[35] A. Olad, F. Doustdar and H. Gharekhani, *Carbohyd. Polym.*, **200**, 516 (2018), https://doi.10.1016/j.carbpol.2018.08.014
[36] X. Hu, X. Jia, C. Zhi, Z. Jin and M. Miao, *Carbohyd. Polym.*, **210**, 204 (2019), https://doi.org/10.1016/j.carbpol.2019.01.043
[37] K. Venkatachalam, N. Rakkapao and S. Lekjing, *Membranes*, **13**, 161 (2023), https://doi.org/10.3390/membranes13020161
[38] P. N. Raju and P. S. Ganguly, *Indian J. Dairy Sci.*, **68**, 316 (2015), https://doi.10.5146/ijds.v68i4.43641
[39] N. Y. Elmehbad, N. A. Mohamed, N. A. Abd El-Ghany and M. M. Abdel-Aziz, *Int. J. Biol. Macromol.*, **246**, 125582 (2023), https://doi.10.1016/j.ijbiomac.2023.125582